PHASE DISPERSION CHARACTERIZATION OF FIBRE GRATINGS

S Barcelos*, M N Zervas, R I Laming and D N Payne

Optoelectronics Research Centre
University of Southampton
Southampton, SO17 1BJ, UK
Fax: +44 1703 593149
Email: S.Barcelos@ieee.org
(*) IEEE/LEOS Member

Abstract

A high wavelength resolution set-up based on an interferometric technique has been used to provide accurate phase dispersion and time delay measurements of fibre photorefractive gratings. Standard and highly chirped gratings has been characterized and the results used to develop a chirped fibre filter which can be used for dispersion-compensation in long fibre telecommunications links, thus greatly enhancing the capacity of the existing fibre base.

1. INTRODUCTION

One of the most important fibre-optic devices to have emerged in the recent years is the fibre grating [1]. It finds applications in DFB and DBR fibre lasers, dispersion compensation and fibre sensors. Full and accurate amplitude and phase (dispersion) characterization of this device is therefore needed. We have demonstrated such a system based on an interferometric technique (figure 1). The reference arm of a fibre Michelson interferometer is phase-modulated with a saw-tooth function to generate an electric signal at the photodetector which carries the optical phase and amplitude information of the reflective fibre device under test (DUT). The amplitude response of the interferometer is directly proportional to the field reflection coefficient, whereas the measured relative phase is related to the time delay response of the device. The set-up is fully automated and uses a Hewlett Packard tunable laser source (1470-1560nm) with wavelength accuracy <0.01nm [2]. A temperature feedback control loop can be used to actively compensate for the temperature-dependent phase drifts in the fibre interferometer arms [3]. The control signal is generated by tracking the phase of a second laser signal (1311nm from a DFB source). In closed loop operation, the phase stability is within ±0.1° and ±5° for the 1311nm and 1550nm detected signals, respectively, over 1 hour. In open loop operation, the phase drifts slowly. Nevertheless, this results only on a small error (<10%) in the time delay data derived from the phase measurements, proving that our system is also suitable for measurements in open loop operation. The phase modulators PM_1 and PM_2 are high resonance piezoelectric ceramic cylinders which are wrapped round with some turns of fibre.

By stepping the input wavelength in small steps $\Delta\lambda$, the phase of the electric signal changes by $\Delta\Theta_v = \Delta\Theta_{DUT}$. The equivalent time delay τ_{DUT} due to the light reflected in the dispersive DUT is given by [4]:

$$\tau_{DUT} = \frac{d\Theta_{DUT}(\omega)}{d\omega} = -\frac{\lambda^2}{2\pi c}\cdot\frac{d\Theta_{DUT}(\lambda)}{d\lambda} \approx -\frac{\lambda^2}{2\pi c}\cdot\frac{\Delta\Theta_v}{\Delta\lambda} \qquad (1)$$

where c is the velocity and λ the wavelength of the light in free space.

2. MEASUREMENT RESULTS AND DISCUSSIONS

The set-up of figure 1 was used to measure the reflection and dispersion characteristics of a short standard (unchirped) as well as a long fibre Bragg grating. The short grating was 0.5mm long and its reflection bandwidth was 1.5nm and the peak reflectivity 49%. The length of the long grating was 20mm. At room temperature, its reflection bandwidth and peak reflectivity were 0.20nm and 77%, respectively. These parameters were measured non-interferometrically, by blocking the reference arm of the interferometer. This long grating was tested first at room temperature, launching light from both its left and right sides, and, second, with a temperature gradient applied to it in order to induce a variable chirp.

Figure 2 shows the measurement results for the short grating. Fig 2(a), in particular, shows the lock-in amplitude which is directly proportional to the reflection coefficient. Fig. 2(b) shows the lock-in phase, which is equivalent to the relative phase response of the grating. The time delay is shown in fig. 2(c). The figures reveal all the basic features of a standard Bragg grating. At the points of zero reflection, the phase jumps by about 180° (fig. 2(b)). Around these points, the slope of the phase curve varies with the wavelength (as seen in the figure insets) which indicates the presence of dispersion. Away from the zero reflection points, the phase increases linearly, which means zero dispersion. This is qualitatively in good agreement with theoretical predictions.

Figures 3-7 are all related to the 20mm long grating. In figure 3, light enters the grating from the left side. Fig. 3(b) demonstrates that the relative phase difference of the reflected light varies non-linearly with wavelength. This corresponds on average to a quasi-linear decrease of the time delay across the reflection bandwidth (negative dispersion) and indicates that shorter wavelengths are delayed more in the reflection process. This clearly demonstrates that the fabricated grating is non-uniform and pre-chirped. The pronounced peaks in the time delay are related to the fibre birefringence and Fabry-Perot-type resonances.

In figure 4, the grating is reversed and light enters from the right side. All features in the reflectivity, phase and time delay plots are very similar to those observed in figure 3. However, phase and time delay variations are reversed. The peaks in the time delay plot point towards the opposite direction and the dispersion in the reflection band is now positive, with shorter wavelengths reflected first.

In order to induce additional chirp, different temperature gradients were applied to the 20mm reversed grating of figure 4. The gradient was achieved by placing the grating in a 25mm long V-groove made on an aluminium slab, and heating its left and right sides with two separate peltier elements. In figure 5, the gradient is approximately constant and the left and right side temperatures are 26.3°C and 26.1°C, respectively. In figure 6, the left and right side temperatures are 25.8°C and 90°C, and, in figure 7, 92°C and 25.5°C, respectively. The results in figure 5 are all comparable to the plots in figure 4 (apart from the scale change) as expected. In figure 6, the grating spectrum broadens and the reflection peak shifts. Also, the dispersion in the reflection bandwidth reduces (but it is still positive). This is because the temperature gradient enhances the initial chirp of the grating. In figure 7, the temperature gradient has been reversed. In this case, the grating spectrum gets narrower and the reflection peak shifts as compared with figure 5. However, the interesting feature is that the dispersion in the reflection band changes sign, indicating that the chirp has changed sign as well. The measured average slope of the time delay is about -560ps/nm, which means that this grating can be very useful for dispersion compensation in telecommunication links as it can compensate the dispersion of about 35-40km of standard fibre.

In all the measurements related to the 20mm long grating (figures 3-7), under different amounts of chirping, we notice that the average total time delay across the full reflection bandwidth of the grating is about 200ps. This corresponds to a fibre length of ~40mm, which, as anticipated, is exactly twice the grating length.

The reversed 20mm long grating was tested in a 2.5Gbit/s transmission system and the Bit Error Rate was measured for different span lengths [5]. From the plots of the receiver penalty due to dispersion versus span length, it was found that, by applying a temperature gradient similar to the one of figure 7, dispersion compensation of about 40km of standard telecom fibre is achieved.

3. CONCLUSIONS

In conclusion we have demonstrated an interferometric technique capable of measuring the dispersion of fibre gratings. We have used it to study chirped fibre gratings for dispersion compensation purposes. We have found that, by applying a temperature gradient of 2.7°C/mm to a **2cm** long grating, we can create a negative dispersion capable of compensating the dispersion of about **35-40km** of standard telecom fibre. The limitations of our interferometric set-up are the wavelength resolution and stability of the tunable laser sources and spurious reflections in splices and other parts of the interferometer. Although they add noise into the measurements, they do not affect the quantitative estimation of the induced dispersion. We have found that our results are very repeatable and in good agreement with the theory [6] and systems measurements.

4. ACKNOWLEDGEMENTS

The authors acknowledge L Reekie for fabricating the fibre gratings. S Barcelos acknowledges the support of the Brazilian National Council for Science and Technology (CNPq) and R I Laming acknowledge the Royal Society for provision of a Research fellowship. This work has been supported by Pirelli Cavi SpA. The ORC is an EPSRC Interdisciplinary Research Centre.

5. REFERENCES

[1] Morey W W, Ball G A and Meltz G, "Photoinduced Bragg gratings in optical fibres", Optics and Photonics News, vol 5, No 2, pp 8-14, February 1994.

[2] Hewlett Packard Tunable Laser Source HP 8168A, equipment specifications.

[3] Barcelos S, "Desenvolvimento de uma Hibrida em Fibra Optica para Receptores Coerentes", Master degree thesis, DMO/FEE/UNICAMP-State University of Campinas, Brazil, March, 1991; also: Barcelos S and Conforti E, "Analise de uma Hibrida de 90° Para Comunicações Opticas Coerentes", Proceedings IV Simposio Brasileiro de Microondas - SBMO, USP, São Carlos, Brazil, July 1990, pp. 115-120.

[4] Senior J M, "Optical Fiber Communications: Principles and Practice", Prentice-Hall, 2nd Ed, 1992, chapter 3, pp. 107-108.

[5] Laming R I et al, paper under preparation.

[6] Zervas M N et al, paper under preparation.

FIGURES

Figure 1: Measurement system. M_1: reference mirror (reflects both 1311 and 1550nm); DUT: device under test, reflects 1550/pass 1311nm; $G_{1,3}$ grating that reflects only 1311nm; PM_1 and PM_2: optical phase modulators; HPWF/LPWF: optical filters that pass 1550nm/1311nm and rejects 1311/1550nm respectively; BPF: electronic bandpass filters centred at the 3rd harmonic of the saw-tooth function.

Figure 2: Experimental results for a 0.5mm long periodic fibre Bragg grating: (a) lock-in amplitude (~ reflection coefficient), (b) lock-in phase and (c) time delay responses.

Figure 3: Experimental results for a 20mm long fibre grating, with light entering from its left side fibre (room temperature = 22°C): (a) square of lock-in amplitude (~ reflectivity), (b) lock-in phase and (c) time delay responses.

Figure 4: Results for the case of reversing the grating, and light entering from the right side fibre (room temperature = 22°C).

Figure 5: Reversed grating with approximately constant temperature gradient applied: left side temperature = 26.3°C, right side temperature = 26.1°C.

Figure 6: Reversed grating with temperature gradient: left side temperature = 25.8°C, right side temperature = 90°C.

Figure 7: Reversed grating with temperature gradient: left side temperature = 92°C, right side temperature = 25.5°C.

Figure 1

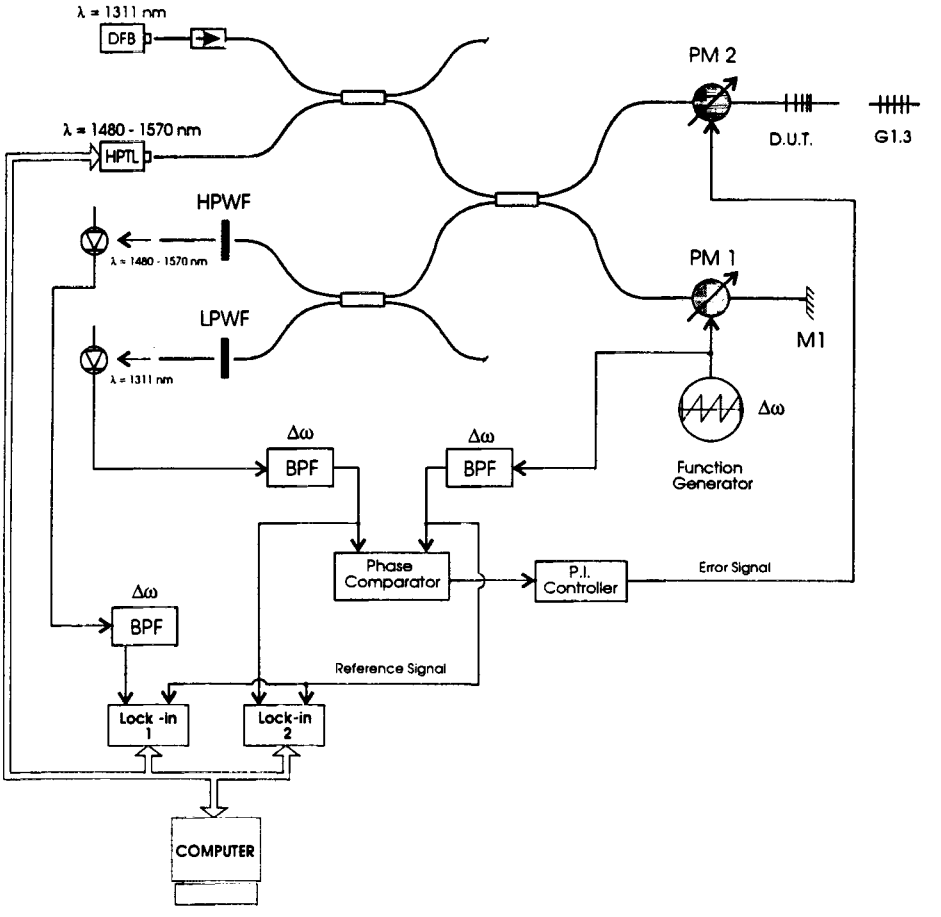

Figure 2

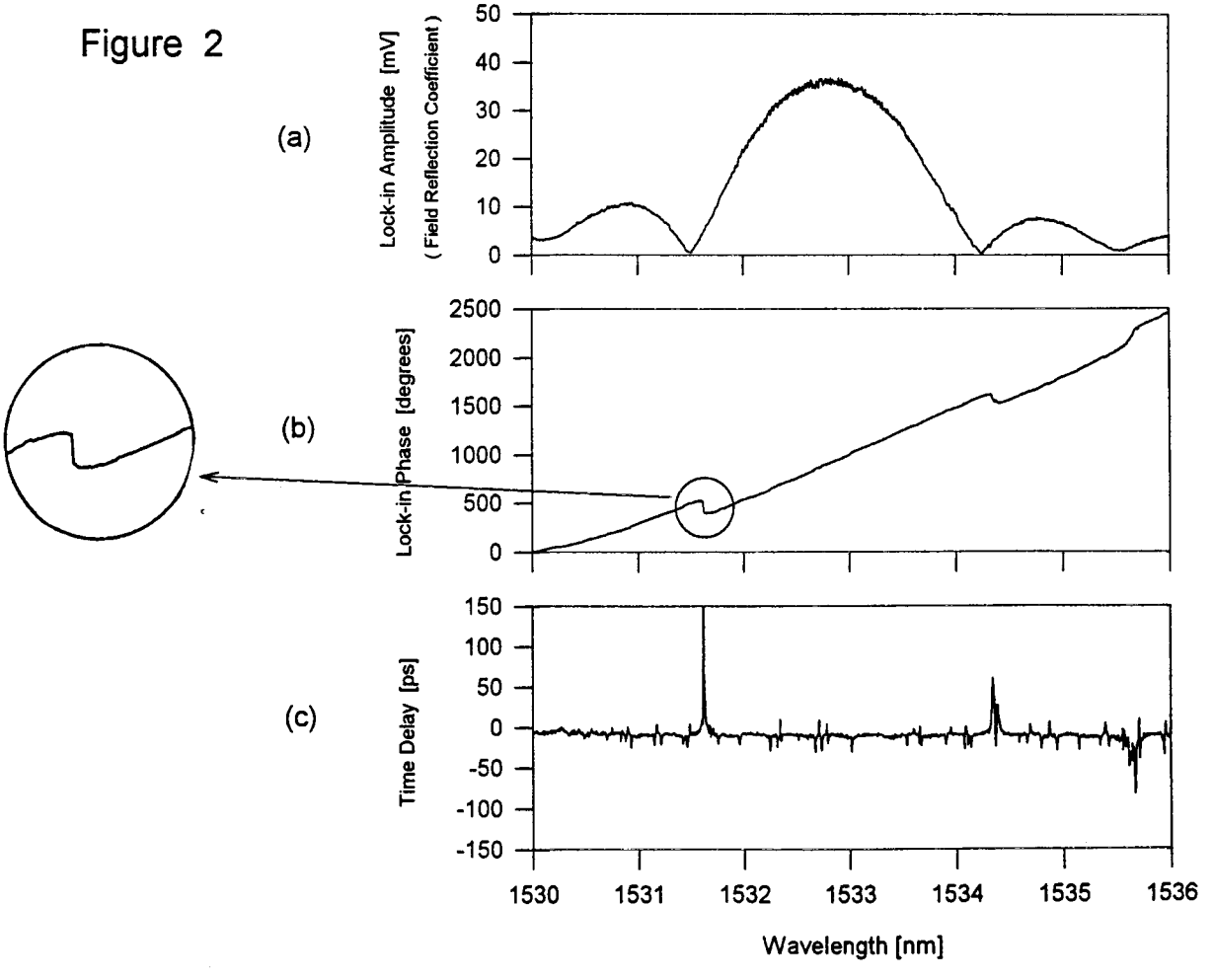

Figure 3

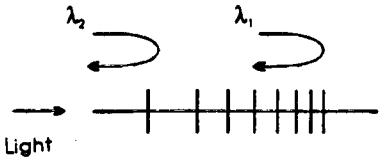

(a)

(b)

(c)

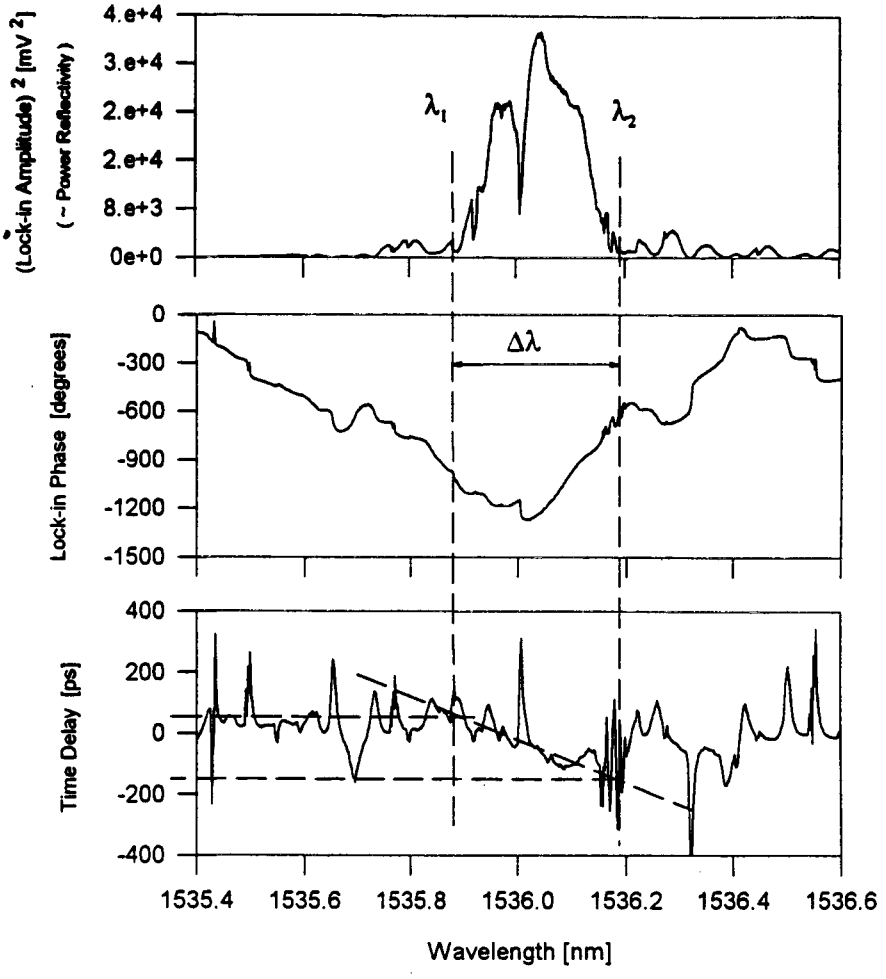

Figure 4

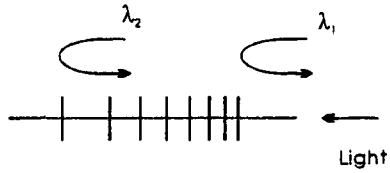

(a)

(b)

(c)

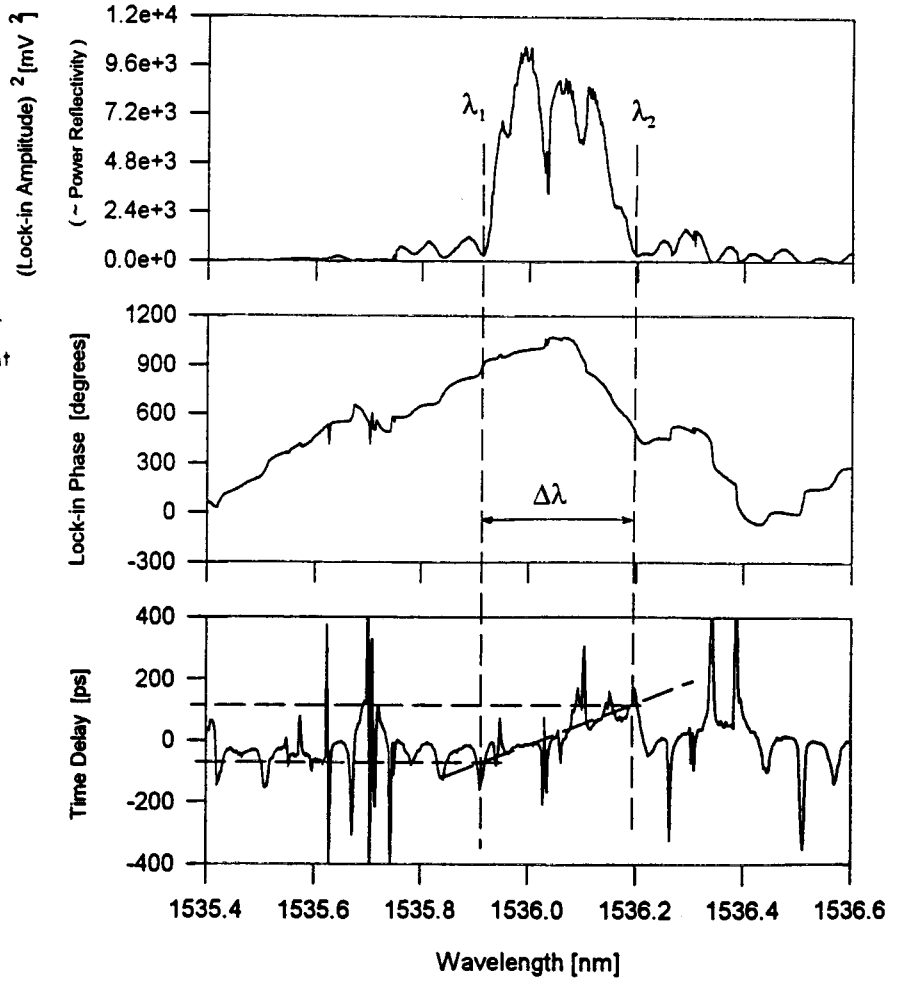

Figure 5

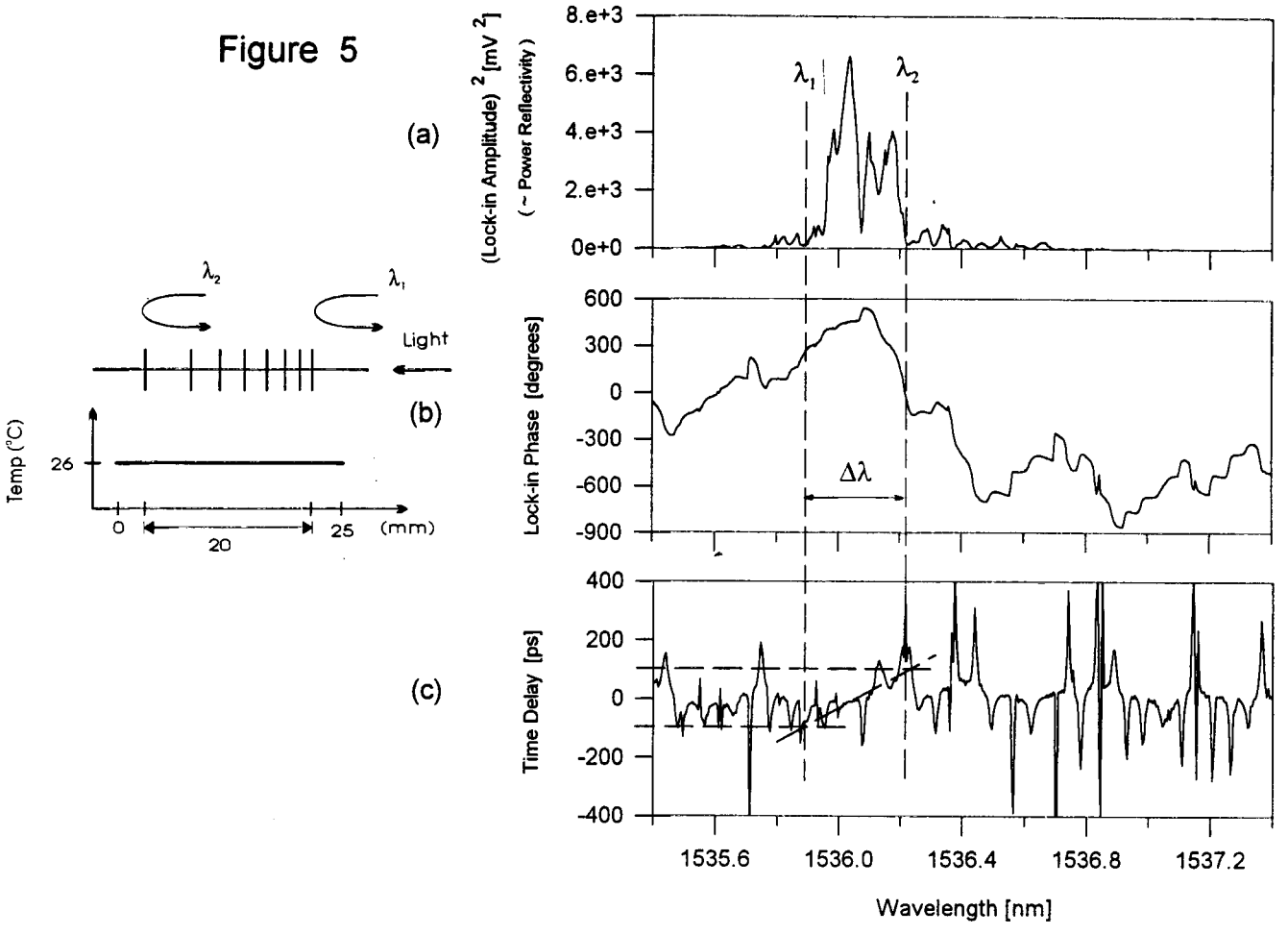

Figure 6

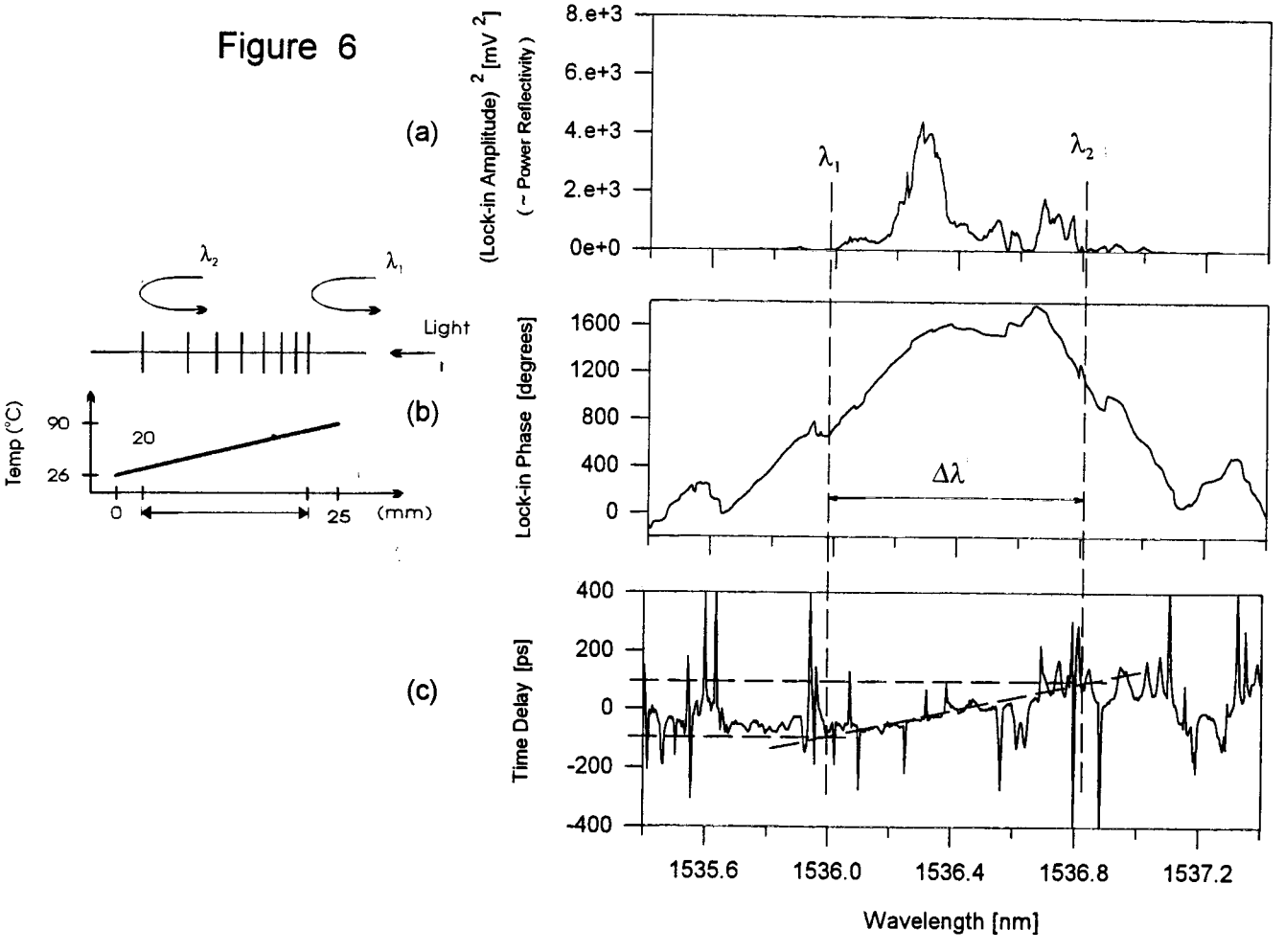

Figure 7

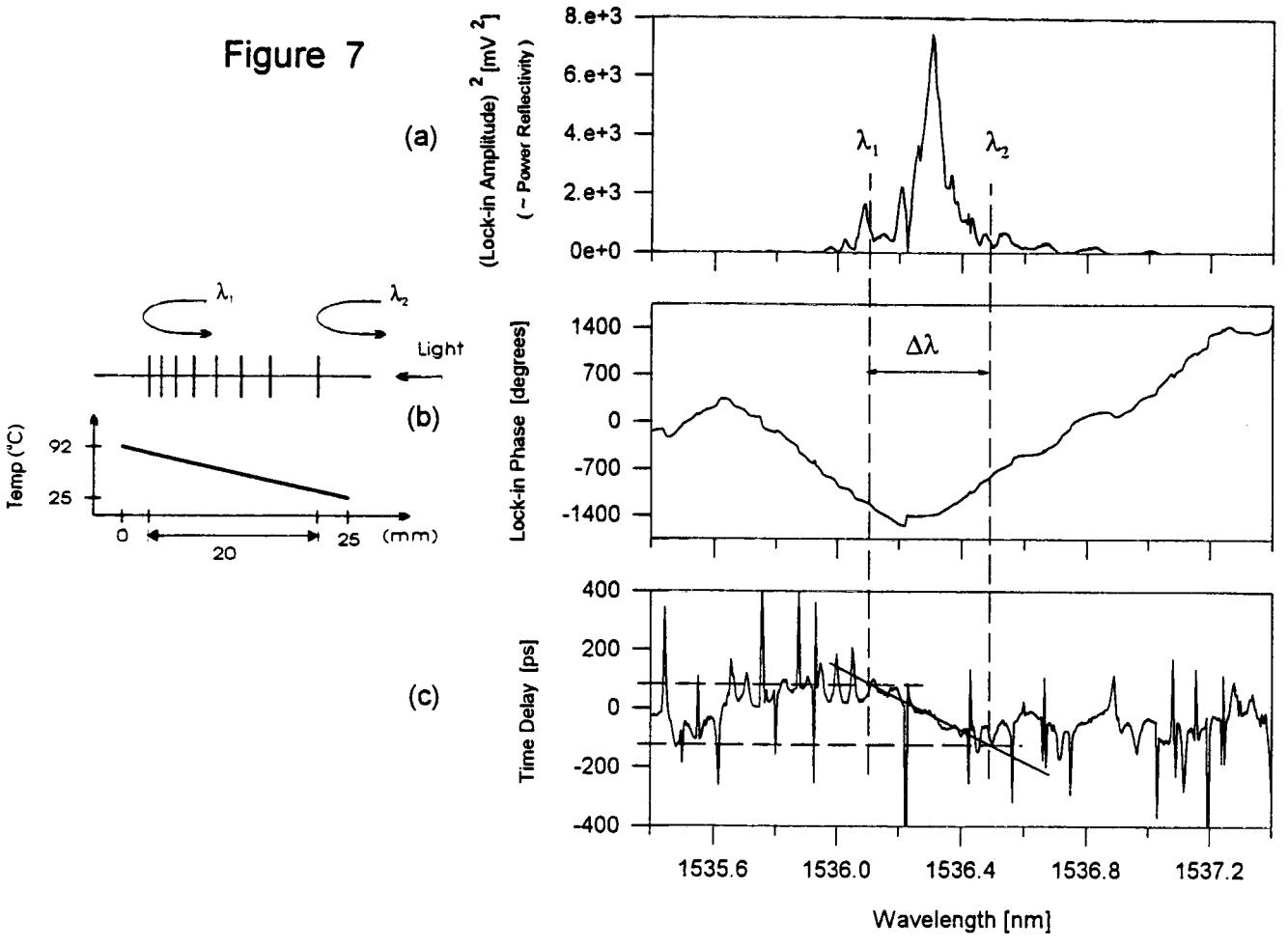
(a)
(b)
(c)
λ1
λ2
Light
Temp (°C)
92
25
0
20
25
(mm)
(Lock-in Amplitude)² [mV²]
(~ Power Reflectivity)
8.e+3
6.e+3
4.e+3
2.e+3
0e+0
Lock-in Phase [degrees]
1400
700
0
-700
-1400
Δλ
Time Delay [ps]
400
200
0
-200
-400
1535.6
1536.0
1536.4
1536.8
1537.2
Wavelength [nm]